Journal of Photopolymer Science and Technology
Volume 21, Number 3 (2008) 357-362 ©2008 CPST

Light Emitting Materials for Organic Electronics

Yun Chi,* and Pi-Tai Chou[±]

Department of Chemistry, National Tsing Hua University, Hsinchu 300, Taiwan
Fax: (+886) 3 572 0864; E-mail: ychi@mx.nthu.edu.tw
[±]Department of Chemistry, National Taiwan University, Taipei 106, Taiwan

This paper presents the case studies on the syntheses and characterization of three third-row transition metal complexes, all of them are associated with at least one functionalized 2-pyridyl pyrazolate chelates. Each of these complexes possesses distinctive central metal atom and shows highly efficient phosphorescent emission ranging from red, green and blue of the visible spectrum. Their photophysical properties are briefly discussed, including the assignment of their fundamental absorption and emission characteristics. Finally, performance data on fabrication of phosphorescent OLEDs using these complexes as emitters are presented.
Keyword: phosphorescence, osmium, iridium, platinum, organic light-emitting diode

1. Introduction

The preparation of heavy transition-metal complexes with Os(II), Ir(III) and Pt(II) central ions is particularly attractive because of their strong metal-ligand interaction, which significantly improves their chemical and electrochemical stabilities. The strong spin-orbit coupling expected for these heavy metal ions would lead to an efficient intersystem crossing from the singlet excited state to the triplet manifold. Furthermore, mixing singlet and triplet excited-states via spin-orbit coupling, to a great extent, would also remove the spin-forbidden nature of the $T_1 \rightarrow S_0$ radiative relaxation, resulting in the highly intense phosphorescent emission. Based on these concepts, the aforementioned transition metal complexes with neutral diimine, anionic cyclometalated or even other tailor-made chelating ligands can give rise to the desirable absorption and efficient emission characteristics [1-4]. More specifically, these chelate complexes would display intense ligand-centered $\pi\pi^*$ absorptions plus a relatively weak, lower energy metal-to-ligand charge transfer (MLCT) transition, while the strong emission is expected to derive from $\pi\pi^*$, MLCT or a mixture of both states, respectively, making them suitable to serve as ideal phosphors for fabrication of organic light emitting devices OLEDs.

Since the manufacture of a full color display requires the usage of emitters with all three primary colors, i.e. blue, green and red, rationally tuning emission color over the entire visible range has emerged as an important task. Similar to their fluorescent counterparts, a systematic variation of the ligands has allowed an accurate prediction of their emission colors; for example, it has been documented that the *tris*-cyclometalated complex $[Ir(ppy)_3]$, ppy = 2-phenyl pyridine, displays a vivid emission at 510 nm and has been widely used as dopant for green emitting phosphorescent OLEDs [5]. Upon changing the pyridyl substituent of ppy ligand to a 1-isoquniolinyl substituent, the resulting *tris*-cyclometalated complex $[Ir(piq)_3]$, piq = 1-phenyl isoquinoline, showed bright red emission at ~620 nm attributed to its much longer elongation of ligand π-conjugation,

Received March 26, 2008
Accepted May 9, 2008

affording [Ir(piq)$_3$] a superb dopant for the red-emitting PhOLEDs [6]. In this article, we like to present the representative studies that allow the successful preparation of red, green and blue-emitting phosphors derived from the heavy transition metal complexes employing functionalized pyridyl pyrazolate chelates as shown below:

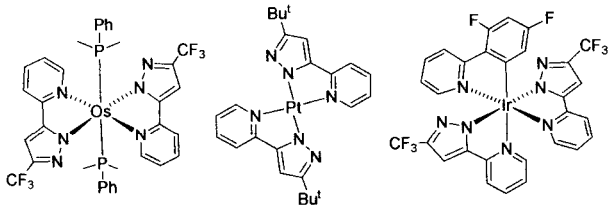

[Os(fppz)$_2$(PPhMe$_2$)$_2$] [Pt(bppz)$_2$] [Ir(dfppy)(fppz)$_2$]

2. Experimental

2.1. General Procedures

All reactions were performed under nitrogen. Solvents were distilled from appropriate drying agent prior to use. Commercially available reagents were used without further purification unless otherwise stated. 3-Trifluoromethyl-5-(2-pyridyl) pyrazole (fppz)H was prepared from reaction of 2-acetylpyridine with either ethyl trifluoroacetate, followed by treatment with hydrazine hydrate in ethanol solution, while 3-*tert*-butyl-5-(2-pyridyl) pyrazole (bppzH) was prepared from reaction involving ethyl picolinate and pinacolone, followed by treatment of the condensation product with hydrazine hydrate under similar conditions [7]. All reactions were monitored by TLC with Merck pre-coated glass plates (0.20 mm with fluorescent indicator UV_{254}). Flash column chromatography was carried out using silica gel from Merck (230-400 mesh). Steady-state absorption and emission spectra were recorded by a Hitachi (U-3310) spectrophotometer and an Edinburgh (FS920) fluorimeter, respectively. Phosphorescence of all metal complexes was recorded under degassed condition using at least three freeze-pump-thaw cycles.

2.2. Preparation of [Os(fppz)$_2$(PPhMe$_2$)$_2$]

To a 50 mL reaction flask was charged with 3-trifluoromethyl-5-(2-pyridyl)-pyrazole (fppzH, 300 mg, 1.4 mmol), pulverized $Os_3(CO)_{12}$ (200 mg, 0.22 mmol), and 20 mL of anhydrous diethylene glycol monoethyl ether (DGME). The mixture was heated at 180 ~ 190°C for 24 hours. After then, the temperature was lowered to ~150°C, freshly sublimed Me_3NO (120 mg, 1.59 mmol) dissolved in 12 mL of DGME was added, and stirring was continued for 5 min. Finally, $PPhMe_2$ (450 mg, 3.26 mmol) was injected into the mixture. In the meantime, the temperature of solution was raised up to 190°C. After 12 hours, the reaction was stopped. The solvent was evaporated under vacuum, and the residue was washed with distilled water (20 mL × 2) to remove the remaining Me_3NO. Purification by silica gel column chromatography (with EA : hexane = 1 : 1 as eluent), followed by recrystallization from a mixture of EA and hexane at room temperature, yielded bright red crystalline solid (443 mg, 0.50 mmol) in 68 % yield.

Spectral data: MS (FAB, ^{192}Os), observed m/z [assignment]: 892 [M^+], 754 [M^+ – $PPhMe_2$], 616 [M^+ – $2PPhMe_2$]. ^{1}H NMR (400 MHz, d_6-acetone): δ 10.31 (dd, 2H, J_{HH} = 6.6, 0.8 Hz, H_{py}), 7.56 ~ 7.48 (m, 4H, H_{py}), 7.05 (ddd, 2H, J_{HH} = 6.8, 6.6, 0.8 Hz, H_{py}), 6.94 ~ 6.87 (m, 8H, H_{Ph}, H_{pz}), 6.42 ~ 6.38 (m, 4H, H_{Ph}), 0.80 (t, 6H, J_{HP} = 3.6 Hz, Me), 0.60 (t, 6H, J_{HP} = 3.6 Hz, Me). ^{19}F NMR (470 MHz, d_6-acetone): δ –59.5 (s). ^{31}P NMR (202 MHz, d_6-acetone): δ –19.6 (s). Anal. Calcd. For $C_{34}H_{32}F_6N_6P_2Os$: C, 45.84; N, 9.43; H, 3.62. Found: C, 46.00; N, 9.32; H, 3.81.

2.3. Preparation of [Pt(bppz)$_2$]

The ethanol solution of 3-*tert*-butyl-5-(2-pyridyl) pyrazole (bppzH, 92 mg, 0.50 mmol) and K_2PtCl_4 (100 mg, 0.24 mmol) was brought to reflux for 12 hours. After that, the solvent was evaporated under vacuum, and 60 mL of CH_2Cl_2 was added to extract the product. The extract was then washed with water, dried over anhydrous Na_2SO_4, and concentrated to dryness, giving a yellowish green powder. Further purification was conducted using vacuum sublimation (160°C, 220 mtorr), affording 80 mg of [Pt(bppz)$_2$] as bright green needles (0.13 mmol, 54%).

Spectral data: MS (EI, 70eV), observed m/z (actual) [assignment]: 595 (595) [M^+]. ^{1}H NMR (400 MHz, $CDCl_3$, 294 K): δ 10.79 (d, J_{HH} = 6.0 Hz, 2H), 7.82 (ddd, J_{HH} = 7.9 Hz, J_{HH} = 7.6 Hz, J_{HH} = 1.2 Hz, 2H), 7.55 (d, J_{HH} = 7.9 Hz, 2H), 7.19 (ddd, J_{HH} = 7.6 Hz, J_{HH} = 6.0 Hz, J_{HH} = 1.2 Hz, 2H), 6.49 (s, 2H), 1.42

(s, 18H). ^{13}C NMR (125 MHz, $CDCl_3$, 294K): δ 161.4 (C_{py}), 155.4 (C_{pz}), 152.3 (CH_{py}), 149.4 (C_{pz}), 138.8 (CH_{py}), 120.7 (CH_{py}), 117.8 (CH_{py}), 99.4 (CH_{pz}), 32.6 ($C_{t\text{-}butyl}$), 31.0 (CH_3). Anal. Calcd. for $C_{24}H_{28}N_6Pt$: C, 48.40; N, 14.11; H, 4.74. Found: C, 48.31; N, 14.10; H, 4.88.

2.4. Preparation of [Ir(dfppy)(fppz)$_2$]

A mixture of 4,6-difluorophenyl pyridine (dfppyH, 0.20 g, 1.07 mmol) and $IrCl_3 \cdot 3H_2O$ (340 mg, 0.97 mmol) in 2-methoxyethanol (20 mL) was refluxed for 4 hours under N_2. The mixture was then cooled to room temperature, followed by addition of 430 mg of fppzH (2.04 mmol) and 450 mg of Na_2CO_3 (4.27 mmol). The resulting mixture was refluxed for another 8 hours, and 20 mL deionized water was added after cooling the solution to RT. The yellow precipitate was collected by filtration. The precipitate was separated using silica gel column chromatography (ethyl acetate : hexane = 1 : 1), giving the blue emissive complex [Ir(dfppy)(fppz)$_2$] (140 mg, 0.17 mmol, 18 %) as the fastest eluting component.

Spectral data: MS (FAB, ^{192}Ir): observed m/z [assignment]: 808 [M^+ + 1]. ^1H NMR (400 MHz, d_6-acetone, 294 K): δ 8.26 (d, J_{HH} = 8.8 Hz, 1H), 8.18 ~ 8.03 (m, 4H), 7.94 ~ 7.90 (m, 2H), 7.44 ~ 7.39 (m, 3H), 7.32 (td, J_{HH} = 5.6, 1.6 Hz, 1H), 7.23 (s, 1H), 7.21 (s, 1H), 7.16 (td, J_{HH} = 6.2, 1.2 Hz, 1H), 6.63 (td, J_{HH} = 8.2, 2.4 Hz, 1H), 5.82 (dd, J_{HH} = 8.8, 2.4 Hz, 1H). ^{19}F NMR (470 MHz, d_6-acetone, 294 K): δ −111.8 (s, 1F), −109.6 (s, 1F), −60.7 (s, 3F), −60.6 (s, 3F). Anal. Calcd. for $C_{29}H_{16}F_8IrN_7$: N, 12.15; C, 43.18; H, 2.00. Found: N, 12.03; C, 43.35; H, 2.02.

3. Results and Discussion

3.1. Red-emitting osmium complexes

This class of red-emitting materials possesses two chelating pyridyl pyrazolates together with two phosphine ligands coordinated to the central Os(II) cation. The pyridyl pyrazolate chelates adopt a mutual trans orientation around the Os(II) center, giving a virtual C_2 symmetry for the whole molecular framework. This conformation is further confirmed by observation of a downfield ^1H NMR signal, attributed to the inter-ligand N···H-C hydrogen bonding occurred between chelating pyrazolates. For its preparation, this Os(II) complex was best conducted using a one-pot synthetic strategy, involving the prior combination of pyridyl pyrazole and the osmium reagent $Os_3(CO)_{12}$, followed by conducting the phosphine substitution to remove the remaining CO ligands in the presence of Me_3NO [8]. This approach circumvents the need for isolation of the dicarbonyl reaction intermediate [9], and hence has an advantage in scaling up for practical application.

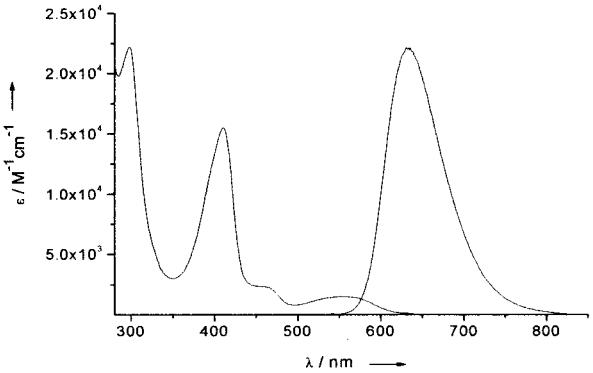

Figure 1. The absorption and emission spectra of [Os(fppz)$_2$(PPhMe$_2$)$_2$] recorded in CH_2Cl_2 solution at RT.

The absorption and luminescence spectra of [Os(fppz)$_2$(PPhMe$_2$)$_2$] are shown in Figure 1, (fppz)H = 3-trifluoromethyl-5-(2-pyridyl) pyrazole. The strong absorption band commonly observed around 411 nm is assigned to the spin-allowed $^1\pi\pi^*$ transition involving the chelating ligands [10]. The next lower energy absorption band around 456 nm can reasonably be ascribed to a spin-allowed metal-to-ligand charge transfer (^{1}MLCT) transition, while the broad peak at 553 nm with lower extinction coefficient (ε = 1600 $M^{-1}cm^{-1}$) is attributed to a heavy atom enhanced, forbidden transition involving both the $^3\pi\pi^*$ and ^{3}MLCT characters. On the other hand, intense luminescence was observed with λ_{max} located at 632 nm in degassed CH_2Cl_2 solution (Φ = 0.19; τ = 0.73 μs). The significant overlap of the 0-0 onsets between emission and the lowest energy absorption band, in combination with a broad, structureless spectral feature, leads us to conclude that the emission originates primarily from the ^{3}MLCT state.

The high efficient phosphorescent OLEDs

has been fabricated by doping this red-emitting Os(II) complex $[Os(fppz)_2(PPhMe_2)_2]$ into poly(*N*-vinyl-carbazole) (PVK) matrix. Upon using 1,3,5-tris(4'-fluorobiphenyl-4-yl)benzene (F-TBB) as a hole-blocking material, maximum luminous efficiencies reached 3.5 cd/A, even with air stable aluminum as the cathode. The CIE 1931 chromaticity coordinates is 0.681, 0.317, and remains unchanged over a wide range of operation voltages [11].

3.2. Green-emitting platinum complexes

The green-emitting Pt(II) complex $[Pt(bppz)_2]$ was best obtained via treatment of the neutral 3-*tert*-butyl-5-(2-pyridyl) pyrazole (bppzH) ligand with K_2PtCl_4 in refluxing ethanol solution [12]. The room temperature UV-Vis and emission spectra in THF solution as well as solid thin film are shown in Figure 2. It is obvious that the strong absorption bands in the UV region (≤ 350 nm) are derived from a typical ligand centered ππ* transition. The lower lying absorption bands have a relatively small extinction coefficient (2200 $M^{-1}cm^{-1}$ at 416 nm and 2100 $M^{-1}cm^{-1}$ at 442 nm) and are tentatively assigned to the transition incorporating a state mixing amongst singlet and triplet metal-ligand charge transfer (^{1}MLCT and ^{3}MLCT) and, to a certain extent, the intra-ligand ^{3}ππ transitions. Interpretation of these MLCT bands may be further complicated by the fact that these bands are clearly composed of two distinctive transitions, for which similar observation has been documented for the Pt(II) acetylide complexes [13]. Moreover, the proximal energy levels between ^{1}MLCT and ^{3}MLCT bands suggest that the ^{3}MLCT transition is greatly enhanced by the spin-orbit coupling and becomes partially allowed.

The fairly intensive emission maximized at 494 nm (Φ = 0.19; τ = 0.4 μs) was observed in degassed THF. The spectral mirror image with respect to the lowest lying absorption profile leads us to conclude that the emission mainly originates from a triplet manifold, while the notable vibronic coupling showed an increased proportion of ππ* transition characters compared with the red-emitting Os(II) complex discussed in previous section. Interestingly, the emission of $[Pt(bppz)_2]$ showed three vibronic peaks at 489, 518 and 550 nm while recorded in the solid state at RT. For a closer comparison, the intensity ratio for these three vibronic peaks is appreciably different from that observed in fluid solution; i.e. the highest energy emission peak undergoes a ~5 nm (207 cm^{-1}) blue shift in the solid state, while other vibronic maxima remain nearly unchanged. This discrepancy may be rationalized by the environmental (inhomogeneous) perturbation on the vibronic peaks, especially the 0-0 onset, in solid film.

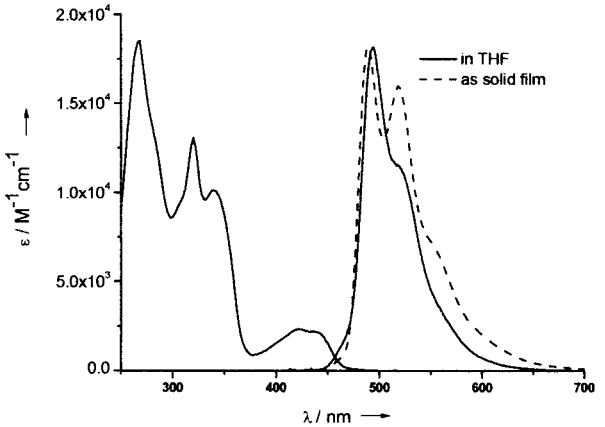

Figure 2. The absorption recorded in THF and the emission spectra recorded in THF solution and as solid thin film.

This Pt(II) complex is also of suitable for fabrication of high performance phosphorescent OLEDs. Multilayer devices of the configuration ITO/NPB(40 nm)/CBP:$[Pt(bppz)_2]$(30nm)/BCP(10 nm)/Alq_3(30 nm)/LiF(1 nm)/Al(150 nm) were prepared, with doping concentrations of $[Pt(bppz)_2]$ varying from 6%, 20%, 50% and to a 100% neat film composition. This device configuration was adopted from those reported by Thompson and Forrest [14]. Excellent device performances were observed for all doping concentrations, including the one with a pure layer of Pt(II) complex. It is important to note that the EL spectra exhibit a large red shift of the emission peak λ_{max} with increasing dopant concentration, from 502 nm, 514 nm, and 518 nm to 556 nm for devices with 6%, 20%, and 50% to 100% of dopant concentration. This may be accredited to the formation of excessive ππ stacking interaction between each of the Pt(II) molecules, despite that the bulky *t*-butyl substituents are capable of suppressing this stacking interaction to a certain degree. Moreover, the higher doping levels gave rise to a much lower initial luminescent quantum yield,

along with a reduced tendency on the driving current.

3.3 Blue-emitting iridium complexes

Preparation of the iridium complex [Ir(dfppy)(fppz)$_2$] was executed by heating of a 1:1 mixture of 4,6-difluorophenylpyridine (dfppy)H and $IrCl_3 \cdot 3H_2O$ in methoxyethanol (140°C, 4 hr), followed by addition of 2.1 equiv. of (fppz)H in presence of Na_2CO_3 (140°C, 8 hr) [15]. This synthetic strategy relies on the prior generation of an intermediate with formula $[(dfppy)IrCl_2]_x$, which would react with the anionic fppz chelate in the subsequent reaction. Figure 3 shows the UV-Visible and emission spectra of [Ir(dfppy)(fppz)$_2$]. In general, the lower lying absorption band (shoulder) with peak wavelengths at 345 ~ 355 nm can reasonably be assigned to a mixed $\pi\pi^*$ and MLCT transition (vide supra).

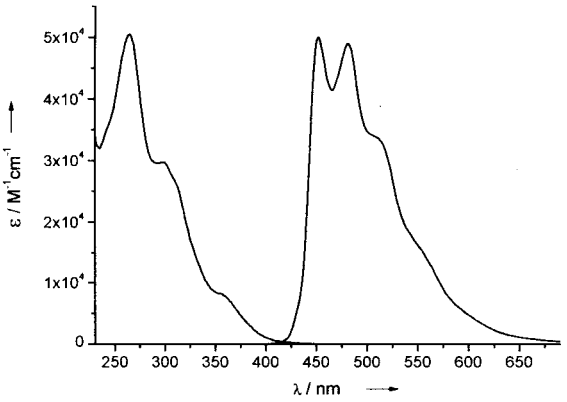

Figure 3. Absorption and luminescence spectra of [Ir(dfppy)(fppz)$_2$] in CH_2Cl_2 solution at room temperature.

In view of emission, [Ir(dfppy)(fppz)$_2$] exhibits strong phosphorescence in solution with an excellent quantum yield (Φ = 0.50), for which four vibronic peaks appeared at ~450, 479, 511 and 554 nm in degassed CH_2Cl_2 solution at 298 K. The lifetime was measured to be 3.8 μs, deducing a radiative lifetime of 7.7 μs. Accordingly, the nonradiative decay rate constant (k_{nr}) is calculated to be 1.30×10^5 s^{-1}. The similarity in k_{nr} leads us to draw the conclusion that the higher emission Q.Y. mainly originates from its shorter radiative lifetime.

Fabrication of electroluminescent devices using [Ir(dfppy)(fppz)$_2$] was carried out in an attempt to achieve true-blue emission. The device configuration consists of ITO/α-NPD (~30 nm)/TCTA (30 nm)/CzSi (3 nm)/CzSi doped with 10 wt.% of [Ir(dfppy)(fppz)$_2$] (25 nm)/UGH2 doped with 10 wt.% of [Ir(dfppy)(fppz)$_2$] (3 nm)/UGH2 (2 nm)/TAZ (50 nm)/LiF (0.5 nm)/Al (150 nm). In this device, double emitting layers (hole-transporting CzSi and electron-transporting UGH2 doped with 10 wt.% of [Ir(dfppy)(fppz)$_2$]) were used to achieve better carrier balance between hole and electron injection/transport and thus to move the exciton formation zone away from the interfaces of both carrier-transport layers. Moreover, a thin UGH2 layer (2 nm) was applied as the buffer layer to prevent the high-energy triplet excitons from migrating to 3-(4-biphenyl)-4-phenyl-5-(4-*tert*-butylphenyl)-1,2,4-triazole (TAZ) that has a lower triplet energy gap. The resulting device exhibits a turn-on voltage of ≤ 4V, a peak external quantum efficiency of up to 8.5% photon/electron, a peak power efficiency of 8.5 lm/W, and a max. brightness of 4000 cd/m^2 at 16 V. Commission Internationale de L'Eclairage (x, y) coordinates ($CIE_{x,y}$) calculated from the EL spectrum are (0.16, 0.18), giving one of the best CIE value and efficiency for deep blue OLED that ever reported in recent literature.

4. Conclusion

In this report, we have demonstrated the successful preparation of three third-row transition metal complexes with suitable emission color and decent quantum yields. Fabrication of phosphorescent OLEDs was achieved in all cases, confirming their potential in future application as emitter dopants for OLEDs. Most importantly, functionalized 2-pyridyl pyrazolate chelates have been successfully employed into these studies, opening an avenue of experimental strategy for the design and construction of highly efficient phosphorescent metal complexes with designated photophysical characteristics.

Acknowledgments

This work was supported by the National Science Council and the Ministry of Economic Affairs of Taiwan.

References

1. R. C. Evans, P. Douglas, and C. J. Winscom, *Coord. Chem. Rev.*, **250** (2006) 2093.
2. P.-T. Chou and Y. Chi, *Eur. J. Inorg. Chem.*, (2006) 3319.
3. P.-T. Chou and Y. Chi, *Chem. Eur. J.*, **13** (2007) 380.
4. Y. Chi and P.-T. Chou, *Chem. Soc. Rev.*, **36** (2007) 1421.
5. A. B. Tamayo, B. D. Alleyne, P. I. Djurovich, S. Lamansky, I. Tsyba, N. N. Ho, R. Bau, and M. E. Thompson, *J. Am. Chem. Soc.*, **125** (2003) 7377.
6. A. Tsuboyama, H. Iwawaki, M. Furugori, T. Mukaide, J. Kamatani, S. Igawa, T. Moriyama, S. Miura, T. Takiguchi, S. Okada, M. Hoshino, and K. Ueno, *J. Am. Chem. Soc.*, **125** (2003) 12971.
7. Thiel, W. R.; Eppinger, J. *Chem. Eur. J.* **3** (1997) 696.
8. Y.-L. Tung, S.-W. Lee, Y. Chi, Y.-T. Tao, C.-H. Chien, Y.-M. Cheng, P.-T. Chou, S.-M. Peng, and C.-S. Liu, *J. Mater. Chem.*, **15** (2005) 460.
9. P.-C. Wu, J.-K. Yu, Y.-H. Song, Y. Chi, P.-T. Chou, S.-M. Peng, and G.-H. Lee, *Organometallics*, **22** (2003) 4938.
10. Y.-L. Tung, P.-C. Wu, C.-S. Liu, Y. Chi, J.-K. Yu, Y.-H. Hu, P.-T. Chou, S.-M. Peng, G.-H. Lee, Y. Tao, A. J. Carty, C.-F. Shu, and F.-I. Wu, *Organometallics*, **23** (2004) 3745.
11. J. Lu, Y. Tao, Y. Chi, and Y. Tung, *Synth. Met.*, **155** (2005) 56.
12. S.-Y. Chang, J. Kavitha, S.-W. Li, C.-S. Hsu, Y. Chi, Y.-S. Yeh, P.-T. Chou, G.-H. Lee, A. J. Carty, Y.-T. Tao, and C.-H. Chien, *Inorg. Chem.*, **45** (2006) 137.
13. C. E. Whittle, J. A. Weinstein, M. W. George, and K. S. Schanze, *Inorg. Chem.*, **40** (2001) 4053.
14. A. Baldo, S. R. Forrest, and M. E. Thompson, *Appl. Phys. Lett.*, **77** (2000) 904.
15. C.-H. Yang, Y.-M. Cheng, Y. Chi, C.-J. Hsu, F.-C. Fang, K.-T. Wong, P.-T. Chou, C.-H. Chang, M.-H. Tsai, and C.-C. Wu, *Angew. Chem. Int. Ed.*, **46** (2007) 2418.